Nonyrast high-spin states in $N=Z$ ^{44}Ti

C. D. O'Leary,[1,2] M. A. Bentley,[2] B. A. Brown,[3] D. E. Appelbe,[1,*] R. A. Bark,[4,†] D. M. Cullen,[1] S. Ertürk,[1,‡] A. Maj,[4,5] and A. C. Merchant[6]
[1]*Oliver Lodge Laboratory, University of Liverpool, Liverpool L69 7ZE, United Kingdom*
[2]*School of Sciences, Staffordshire University, College Road, Stoke-on-Trent ST4 2DE, United Kingdom*
[3]*Department of Physics and Astronomy and the National Superconducting Cyclotron Laboratory, Michigan State University, East Lansing, Michigan 48824*
[4]*Tandem Accelerator Laboratory, Niels Bohr Institute, Risø, DK-4000 Roskilde, Denmark*
[5]*Niewodniczanski Institute of Nuclear Physics, 31–342 Krakow, ul. Radzikowskiego 152, Poland*
[6]*Theoretical Physics, 1 Keble Road, Oxford OX1 3NP, United Kingdom*
(Received 24 January 2000; published 18 May 2000)

High-spin states have been investigated in the $N=Z=22$ nucleus ^{44}Ti. A newly observed set of states with $J^{\pi}=6^{+}$, 8^{+}, 10^{+}, and 12^{+} are assigned to be members of a band built upon an excited 0^{+} state. This band displays rotational-like level spacings, with a near-linear $J(J+1)$ dependence. A third set of $J^{\pi}=8^{+}$, 10^{+}, and 12^{+} states have also been tentatively assigned and a negative-parity intruder band has been extended to $J^{\pi}=13^{-}$. Comparisons with df-shell model calculations show a good agreement for both energy levels and branching ratios. These calculations indicate that the excited 0^{+} band is dominated by a mixture of $8p$–$4h$ and $6p$–$2h$ configurations relative to ^{40}Ca.

PACS number(s): 23.20.Lv, 27.40.+z, 21.60.Cs, 21.60.Gx

I. INTRODUCTION

There has been much contemporary interest in neutron-deficient nuclei within the $f_{7/2}$ shell, particularly those around the $N=Z$ line and near the center of the shell. These nuclei exemplify the interplay between different phenomena [1] as they have a sufficient number of valence quasiparticles to demonstrate collective effects, while also being deficient enough to exhibit properties associated with single-particle behavior.

Work by Simpson *et al.* [2] on ^{44}Ti suggested that in addition to the yrast nonrotational ground-state band there exist three rotational bands based upon excited 0^{+}, 2^{+}, and 3^{-} states. These authors suggested [3] that ^{44}Ti can behave as a soft asymmetric rotor, but that further work was required to see if these bands extend to high spins. In-beam gamma-ray spectroscopy along the $N=Z$ line has advanced significantly in recent times due to the implementation of large arrays of hyperpure Germanium detectors. The use of these arrays in conjunction with devices for detecting particle residues has further enriched the search for high-spin phenomena in medium-mass self-conjugate systems. The primary aim of this work was therefore to re-examine ^{44}Ti at high spin in order to extend the above mentioned bands and to compare any new structures with shell-model calculations.

Titanium-44 has two protons and two neutrons outside the doubly magic nucleus ^{40}Ca. One approach to modeling this nucleus uses a standard spherical-shell basis with four nucleons in a $f_{7/2}$ or $f_{7/2},p_{3/2},f_{5/2},p_{1/2}$ model space; these will be abbreviated by f and fp, respectively. To take into account excitations out of the sd closed shell, the $d_{3/2},f_{7/2}$ (df) model space has been used. This approach assumes eight nucleons outside of a ^{32}S core. We compare our results to shell-model calculations in all these model spaces. In addition a more macroscopic approach is mentioned, where ^{44}Ti is treated as a doubly magic ^{40}Ca core plus one alpha particle. The motivation for this is provided by the considerable success of a cluster model description of the analogous alpha particle plus doubly closed shell core nucleus ^{20}Ne. There, a good description was given of the spectra, enhanced $E2$ transition rates and alpha decay widths, as well as the elastic scattering of alpha particles [4,5]. The application of such a model to ^{44}Ti (see, for example, Merchant *et al.* [6] and references therein) is much less conclusive since the proposed alpha cluster states have erratic energy spacings, rather poorly known electromagnetic properties, and there are no data at all on alpha emission widths. It must be noted, however, that these calculations have been compared with results from experimental work utilizing light-ion reactions such as (α,γ) [2] with low cross sections for the population of high-spin states. Here we use a compound-nucleus, heavy-ion fusion evaporation reaction in conjunction with high-efficiency gamma-ray detectors and ancillary detectors to test for cluster states at high spin in ^{44}Ti.

II. EXPERIMENT

The reaction ^{24}Mg(^{28}Si,2α)^{44}Ti, at a beam energy of 87 MeV upon a 0.5 mg/cm^2 enriched ^{24}Mg target, was studied using the PEX detector apparatus at the Niels Bohr Institute Tandem Accelerator Laboratory. Gamma rays were detected in four EUROBALL cluster detectors [7], with one pair of Germanium clusters mounted at an angle of 104.6° relative to the beam direction and the other pair at 145.8°. A 4π

*Present address: Department of Physics and Astronomy, McMaster University, Hamilton, Canada L8S 4M1.
†Present address: Department of Nuclear Physics, Research School of Physical Sciences and Engineering, Australian National University, Canberra, ACT 0200, Australia.
‡Present address: Nigde Universitesi, Fen-Edebiyat Fakültesi, Fizik Bölümü, Nigde, Turkey.

silicon-wafer array with 31 detector elements [8] surrounding the target was used to detect charged particles, with discrimination between protons and alphas achieved through a comparison of the energy loss of incident particles within each detector element. An array of neutron detectors were mounted at the front of the apparatus.

A software gate was used to select events in which two alpha particles (no protons and no neutrons) were detected, and these were used to build one $\gamma\gamma$-coincidence matrix and two angular correlation matrices. These two angular matrices provided information on the gamma-ray multipolarities, as in these matrices events from either detector angle were incremented on the *x* axes while angle-specific events were incremented on the *y* axes. The ratio of peak areas from the total projection of the *y* axis of one matrix to that of the other are an indication of the angular distribution of different multipoles. Hence it was possible to discriminate between $J \rightarrow J - 2$ (stretched quadrupole) and $J \rightarrow J-1$ (stretched dipole) though not between $J \rightarrow J$ (nonstretched dipoles) and $J \rightarrow J - 2$ transitions. Identical procedures were performed on transitions of known multipolarity in nuclei populated via other reaction channels to test this method.

A gold stopper foil was mounted on the inner surface of the front-most face of the silicon array, 11.5 mm from the target. The recoiling ^{44}Ti nucleus had a velocity of around 13 mm/ns such that any states that decay after a few nanoseconds had a probability of decaying either when the nucleus was in flight or when the nucleus had come to rest in the gold foil. As the gamma-ray spectra were Doppler corrected assuming that the states decay in flight, peaks from gamma transitions from such states had three components—one at the correct energy corresponding to decays in flight and two other components with higher energies corresponding to decays which had occurred after the nucleus had stopped (one component from each cluster-detector angle).

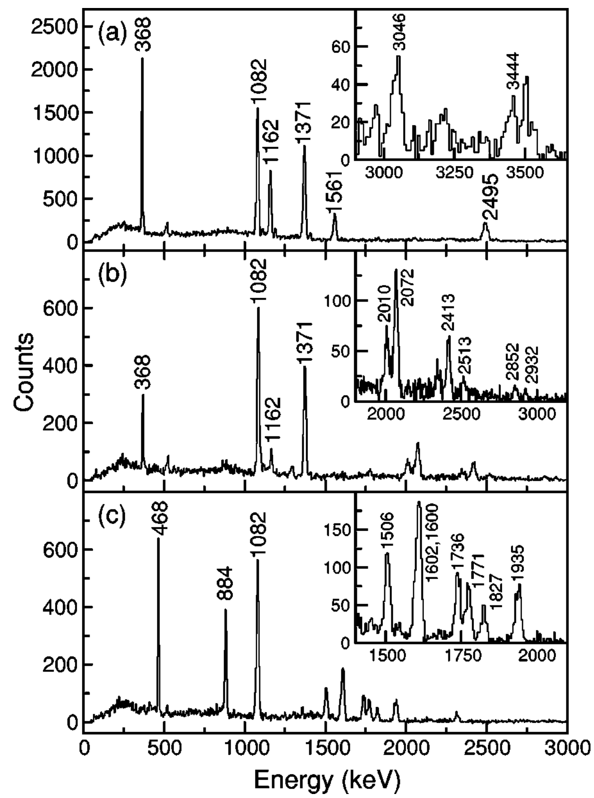

FIG. 1. (a) A sum of spectra gated on the 1561- and 2495-keV gamma rays, the inset shows an expanded region between 2.90 and 3.65 MeV at 8 keV per channel. (b) A spectrum gated on the 2046-keV gamma ray with the inset showing an expanded region between 1.8 and 3.2 MeV, both at 4 keV per channel. (c) A gate on the 2090-keV gamma ray with inset showing an expanded region between 1.4 and 2.1 MeV, both at 4 keV per channel.

III. RESULTS

Spectra in coincidence with combinations of gamma-ray transitions in ^{44}Ti are shown in Fig. 1. Coincidence relationships and intensity measurements were used together with angular distribution information to construct a level scheme for ^{44}Ti as shown in Fig. 2.

Simpson *et al.* [2,3] and Kolata *et al.* [9] had established the ground-state band of ^{44}Ti up to 12^+ at 8 MeV, with states at 1082 (2^+), 2453 (4^+), 4014 (6^+), 6509 (8^+), 7671 (10^+), and 8039 (12^+) keV. These states were observed in this work too. The state at 11 085 keV which feeds directly into the state at 12^+ is tentatively assigned as (14^+).

New gamma ray transitions of energy 2046, 2072, 2413, and 2513 keV have been observed in this work. They are in coincidence with one another, and feed into the ground-state band at the 4^+, 2453 keV state. Angular distribution ratios indicate that these are all stretched $E2$ transitions. It is therefore suggested that a second set of 6^+, 8^+, 10^+, and 12^+ states have been observed at 4499, 6571, 8984, and 11 496 keV, respectively. The possibility of the 2046- and 2072-keV gamma rays being unstretched dipoles is not allowed through the existence of the 1100- and 2010-keV gamma rays which would both have to be $E4$ transitions in this case.

It was possible to observe stopped components of the gamma decays below the $J^{\pi}=12^+$ state at 8039 keV, which has a (previously measured [10]) lifetime of 2.1 ± 0.4 ns. The newly observed 1100-, 2010-, 2046-, and 2072-keV peaks all have stopped components, confirming their position in the level scheme of Fig. 2. Also, stopped events represented a greater portion of the 1100- and 2010-keV gamma rays than the 2072- and 2046-keV, indicating that these latter two proceed mainly via fast components.

The second set of 0^+, 2^+, and 4^+ states were placed by Simpson *et al.* [2] at 1905, 2531, and 3365 keV, respectively. In this work we observe a very weak 1134-keV transition in coincidence with the 2072-, 2413-, and 2513-keV gamma rays (but not with the 2046-keV transition) and propose this 1134-keV gamma ray connects the second 6^+ state to the second 4^+, 3365-keV state. This 1134-keV gamma ray has also been observed in a parallel study [11]. In previous work [2] the 3365-keV state is shown to be linked to the second 2^+ and 0^+ states by a cascade of 834- and 626-keV $E2$ gamma rays. Combining this information, we propose that the newly observed states extend a structure built upon an excited 0^+ state at 1905 keV to 12^+ at 11 496 keV.

The statistics of the present experiment were too weak to obtain convincing angular distribution ratios for the decays

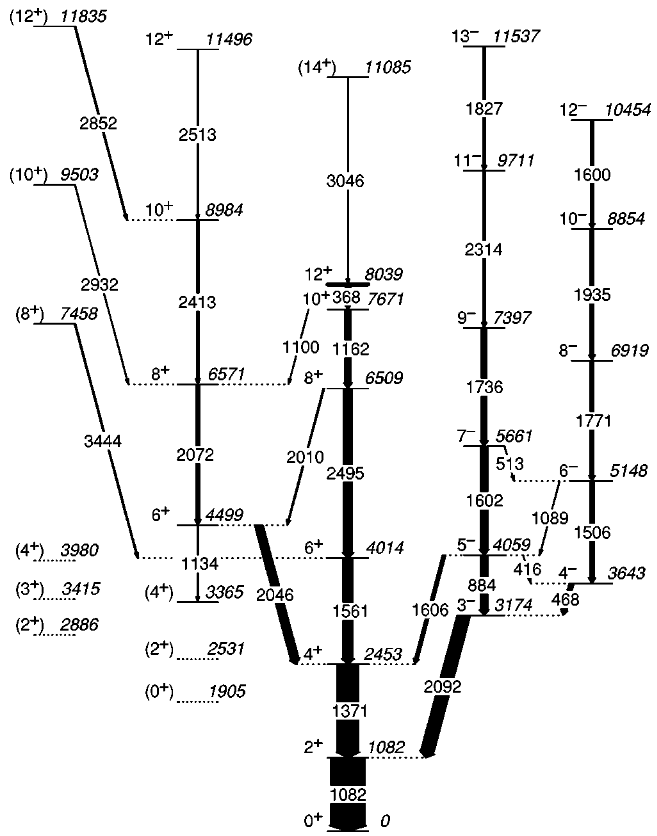

FIG. 2. Energy level scheme deduced from this experiment for ^{44}Ti. The levels are labeled with the assigned spin and parity as well as the excitation energy in keV, with widths of arrows proportional to relative gamma-ray intensity. Bracketed spin assignments are tentative. The states at 1905, 2531, 2886, 3415, and 3980 keV, observed by Simpson *et al.* [2], have not been observed in this work and are shown here as an aid.

from the states at 7458, 9503, and 11 835 keV, but the suggestion is that they are a third set of 8^+, 10^+, and 12^+ states. There is no experimental evidence to link these states with the other rotational-like band observed by Simpson *et al.* [2] with energies (spins) of 2886 keV (2^+), 3415 keV (3^+), and 3980 keV (4^+), which were not observed in this work.

The band built upon the 3^- state at 3174 keV was observed in the present work and has been extended to $J^\pi = 13^-$. The 884-, 1602-, 1736-, 2314-, and 1827-keV transitions are seen to be in coincidence and all display stretched-quadrupole characteristics. It is believed that they are one-half of a signature-split structure, with $E2$ transitions of 1506, 1771, 1935, and 1600 keV forming the other half. This type of signature-split intruder band is a common feature of nuclei in the lower half of the $f_{7/2}$ shell (e.g., ^{46}V [12]).

IV. DISCUSSION

The new level scheme of Fig. 2 is compared with three sets of calculations in different model spaces, carried out with the shell-model code OXBASH. Figure 3(a) represents results [13] using a $f_{7/2}$ only space. The second set of results in Fig. 3(b) are an extension into a full-fp model space using the FPD6 two-body interaction of Richter *et al.* [14].

In Fig. 3(a) the predicted energies for the nonyrast 0^+, 2^+, and 4^+ states are much too high; increasing the valence space to include the full fp shell [Fig. 3(b)] results in a moderate improvement in the energies. Also the nonyrast states are calculated to decay primarily to the yrast band, which does not agree with the band structure observed in the experiment. Due to the lack of success in reproducing the excited bands using the above model spaces, we have also performed calculations in a df valence space. Figure 4 shows level schemes developed from the results of a shell model calculation in a df model space using the two-body interaction of Hsieh *et al.* [15]. A small adjustment was made to the df Hamiltonian by lowering the $d_{3/2}$–$f_{7/2}$ gap by 0.5 MeV and multiplying the Hamiltonian matrix elements by 0.9. Figure 4(a) indicates the relative magnitude of the $B(E2)$s between states. In Fig. 4(b) information on the energy of the gamma rays is included such that the arrow widths represent the fraction of the total $(E2)$ decay probability of a particular transition from each state. This results in a predicted level scheme that has high similarity to the experimental scheme of Fig. 2; note in particular the reproduction of feeding patterns in and around the excited 0_2^+ band and the strong decay out of the band at 6_2^+ to the ground-state band.

The df wave functions for ^{44}Ti can be expanded in terms of the partitions $(d_{3/2})^{(8-k-p)}(f_{7/2})^{(n_v+k+p)}$, where $n_v=4$, $p=0$ for positive parity and $p=1$ for negative parity. When the Hamiltonian is restricted to its spherical single-particle part, the positive-parity ground-state band and the lowest negative-parity band are purely $k=0$. The two-body interaction connects partitions which differ in k value by two units and the resulting states are mixtures of the k partitions. The mixed df wave functions for ^{44}Ti are shown in Table I (the $k \geqslant 6$ components are small for all of these). One finds that the lowest states of each spin are indeed dominated by $k=0$ ($4p-0h$ relative to ^{40}Ca), except for the (14^+) state whose $k=0$ configuration is not allowed. The mixing with the $k=2$ values is large and uniform for all of these states. This type of mixing within the df space has been discussed previously for ^{40}Ca [15,16] and ^{39}Ca [17]. The collectivity of the positive-parity ground-state band is better described by the full $(fp)^4$ configurations, and one might regard the higher k admixtures as part of what influences the effective Hamiltonian in the fp model space.

For the nonyrast states we have to take into account explicitly the excitations out of the sd shell. The df model space gives a "skeleton" picture of what these wave functions are like, but the complete model must eventually also take into account the full sd and fp shells. The nonyrast positive-parity states are dominated by the $k=4$ ($8p-4h$) configuration for low-spin and then change over to a $k=2$ ($6p-2h$) dominance at high spin.

We note that the one-body electromagnetic operator can only connect components of the wave functions with the same k value. The second 6^+ state has an unusually large $k=0$ component related to the mixing with the relatively low-lying second $(f_{7/2})^4$ 6^+ state [13], and this mixing is

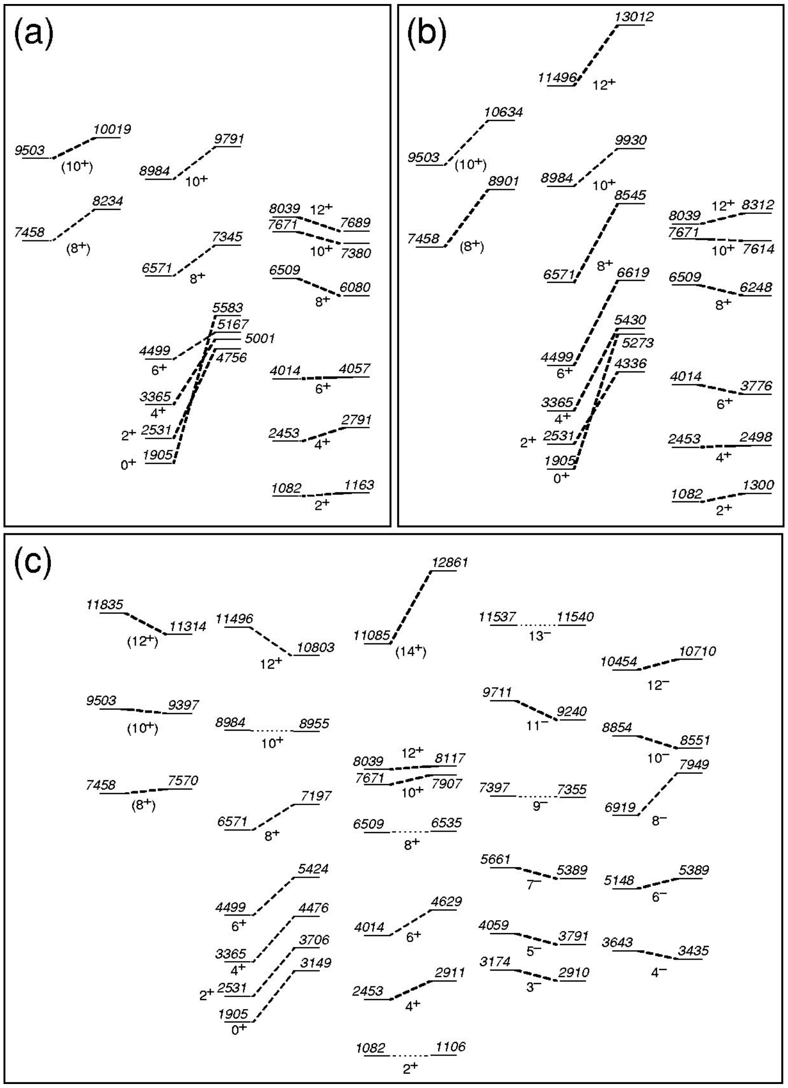

FIG. 3. Comparison between experimental level energies and (a) *f*-shell model calculations [13], (b) fp-shell model calculations. (c) df-shell model calculations. In all cases the levels are grouped by band as in Fig. 2, with experimental energies on the left of each pair, theoretical predictions on the right.

the reason why the nonyrast 0_2^+ band decays to the yrast band at this point. It is also the reason for the sharp increase in rotational frequency at $J \approx 6$ in Fig. 5(a), which compares the variation of angular frequency ω with spin J for the new band with the df-shell model results and the alpha-cluster calculations of Michel *et al.* [5]. This jump is exhibited by the df-shell model results, and probably corresponds to the sudden large overlap between the excited band wave function and that of the ground-state band, the two presumably corresponding to different shapes, as discussed in more detail below.

Titanium-44 is an $N=Z$ nucleus, such that isovector $M1$ transitions are isospin forbidden between its $T=0$ states. As the isoscalar $M1$ components are relatively weak, transitions throughout the nucleus are dominated by their $E2$ components. As in the neighboring $N=Z$ case of ^{46}V [12], this is most readily demonstrated in the negative-parity band where only very weak transitions are observed experimentally between the two signature-split structures.

Figure 5(b) shows the variation of excitation energy with spin of the yrast band, the nonyrast 0_2^+ band and the alpha cluster calculations. This plot shows that this band has energy-level systematics more similar to the alpha-cluster model calculations than the ground-state band. However, the df shell model calculations show that the ground-state band of ^{44}Ti is similar in structure to the ^{40}Ca ground state ($n_v = 0$) with 68.0% $k=0$, 26.2% $k=2$, and 4.9% $k=4$. The ground-state band in ^{44}Ti has a large overlap with ^{40}Ca plus a four nucleon cluster configuration, while that of the nonyrast states is very small. It seems that the strong similarity between the energy-level structure of the 0_2^+ band and the alpha cluster calculations is mere coincidence—though we note that in the work of Hindi *et al.* [18], evidence is shown for $8p-4h$ states in ^{20}Ne with ^{12}C$+^8$Be cluster characteristics.

Recent work on the odd-odd $N=Z$ nucleus ^{46}V [12] indicated the coexistence of prolate-deformed and spherical shapes. Bands exhibiting rotational-like level spacings corresponding to a prolate shape with $\beta \approx 0.3$ and $\gamma \approx 15°$ were found to coexist with a spherical structure, the latter of these being yrast. Zheng *et al.* [19] have searched for highly deformed many-particle–many-hole states in ^{44}Ti using a fixed configuration deformed Hartree-Fock approach with a Skyrme interaction. They predict a low-lying (6.0 MeV)

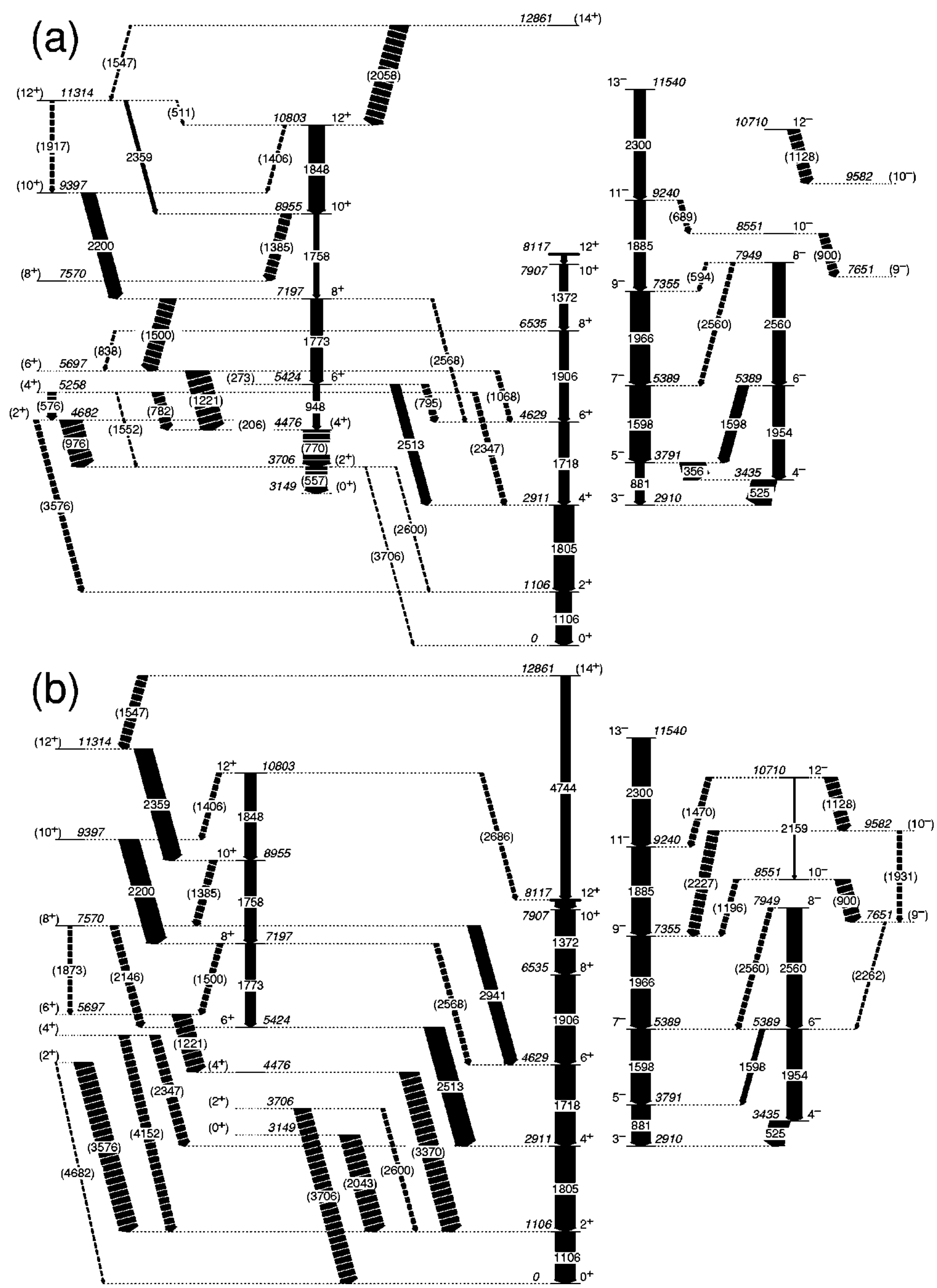

FIG. 4. Energy level schemes for ^{44}Ti deduced from df shell model calculations. The levels are labeled with the assigned spin and parity as well as the excitation energy in keV. Dashed states and transitions have not been confirmed in this experiment. (a) Indicates the relative magnitude of the $B(E2)$s between states, the widths of the arrows being proportional to $B(E2)$ values. Only major transitions $[B(E2) > 10\ e^2\,\mathrm{fm}^4]$ are shown. (b) Indicates where the $E2$ transition strength from a given state is divided, the widths of the arrows are proportional to the branching ratio of each transition. Only major transitions (branching ratio $>\%5$) are shown.

$6p-2h$ state with $\beta=0.29$ and (5.6 MeV) $8p-4h$ with $\beta=0.41$. We have taken a simplistic approach to estimating the deformation of the 0_2^+ band by using these deformations for $k=2$ and $k=4$ and assuming that of the $k=0$ configuration is 0, then weighted them with the partition values from Table I and plotted these as a function of spin in Fig. 5(c). The features of this plot and Fig. 5(d), where we have plotted the dynamic moment of inertia of the 0_2^+ band against spin, are qualitatively similar. A rise at low spins is followed by a sharp drop at around 6^+ where strong mixing with the (low deformation) yrast ground-state band occurs, then a rise up to 12^+. Hence a drop in deformation at around $J^\pi=6^+$ gives rise to the jump in rotational frequency shown in Fig. 5(a) as nuclear angular momentum is conserved.

V. SUMMARY

Nonyrast bands have been established up to high spin in ^{44}Ti. One of these, built upon an excited 0^+ state, displays

TABLE I. Wave function partitions (%) of the df states in ^{44}Ti.

J^{π}_{n}	$k=0$	$k=2$	$k=4$
0^+_1	55.3	36.1	8.1
2^+_1	61.8	32.4	5.6
4^+_1	64.8	30.3	4.8
6^+_1	65.6	30.7	3.5
8^+_1	75.1	22.3	2.5
10^+_1	76.2	21.8	1.9
12^+_1	78.6	19.8	1.6
14^+_1	0.0	81.2	18.5
0^+_2	27.8	21.6	47.3
2^+_2	18.7	36.4	42.6
4^+_2	12.1	47.1	39.2
6^+_2	43.9	40.9	14.8
8^+_2	0.6	71.4	27.0
10^+_2	2.3	85.5	4.8
12^+_2	14.9	84.7	14.9
6^+_3	2.5	88.3	9.0
8^+_3	2.9	87.8	9.2
10^+_3	1.1	84.1	14.3
12^+_3	5.7	65.9	28.0
3^-_1	65.5	32.9	1.6
4^-_1	64.9	32.0	2.4
5^-_1	64.5	32.7	2.8
6^-_1	72.6	25.9	1.5
7^-_1	69.1	28.9	2.0
8^-_1	74.5	24.3	1.1
9^-_1	74.6	24.0	1.4
10^-_1	84.5	14.8	0.6
11^-_1	81.3	17.8	0.9
12^-_1	76.4	23.0	0.6
13^-_1	77.5	21.6	0.9

rotational-like energy-level spacings. Shell model calculations in a df-valence space reproduce the energy-level scheme including feeding patterns very well for all the structures observed. Furthermore, they show the rotational-like 0^+_2 band to be a mixture of $8p-4h$ and $6p$–$2h$ configurations at low spins, with the latter dominant at high spins. As a matter for future interest, Zheng *et al.* [19] have also predicted configurations of $12p-8h$ (at 12 MeV) in ^{44}Ti with $\beta=0.813$ and $16p-12h$ (at 20 MeV) with $\beta=0.985$. It would be intriguing to test this nucleus for such hyperdeformed shapes.

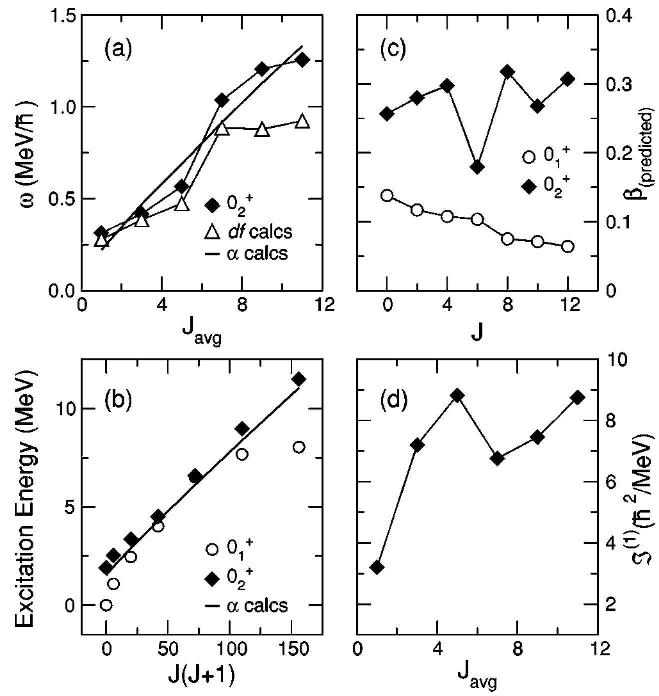

FIG. 5. (a) J versus ω plot, where $J_{avg}=(J_i+J_f)/2$ and $\omega=(E_i-E_f)/2$ for the 0^+_2 1.905 MeV band, the predictions of the df-shell model calculations (see Fig. 4) and the alpha-cluster model of Michel *et al.* [5]. (b) A plot of excitation energy of the ground-state band (circles), the 0^+_2 band (diamonds) and the alpha cluster calculations against spin. (c) A plot of the predicted deformation β for the 0^+_1 and 0^+_2 bands using deformations of 0 for $k=0$, 0.29 for $k=2$, and 0.41 for $k=4$ (from Zheng *et al.* [18]) weighted with the partition values from Table I. (d) A plot of dynamic moment of inertia $\Im^{(1)}$ versus spin for the 0^+_2 band.

ACKNOWLEDGMENTS

The authors are very grateful to Shigeou Ohkubo for helpful advice and Francis Michel for providing numerical values from his calculations. We also acknowledge those responsible for all aspects of the PEX collaboration. This work was supported by the United Kingdom Engineering and Physical Sciences Research Council (EPSRC) from whom Duncan Appelbe received support and by the Danish Natural Science Research Council. B. A. Brown acknowledges support from NSF Grant No. PHY-9605207. Adam Maj is grateful to the Polish State Committee for Scientific Research for partial financial support (KBN Grant No. 2P03B00116).

[1] C. D. O'Leary, M. A. Bentley, D. E. Appelbe, D. M. Cullen, S. Ertürk, R. A. Bark, A. Maj, and T. Saitoh, Phys. Rev. Lett. **79**, 4349 (1997).
[2] J. J. Simpson, W. R. Dixon, and R. S. Storey, Phys. Rev. Lett. **31**, 946 (1973).
[3] J. J. Simpson, W. Dunnweber, J. P. Wurm, P. W. Green, J. A. Kuehner, W. R. Dixon, and R. S. Storey, Phys. Rev. C **11**, 1828 (1975).
[4] A. Arima, H. Horiuchi, K. Kudobera, and N. Takigawa, Adv. Nucl. Phys. **5**, 345 (1972).
[5] F. Michel, G. Reidemeister, and S. Ohkubo, Phys. Rev. Lett. **57**, 1215 (1986); F. Michel (private communication).

[6] A. C. Merchant, K. F. Pál, and P. E. Hodgson, J. Phys. G **15**, 601 (1989).
[7] J. Eberth, P. von Brentano, W. Teichert, H. G. Thomas, A. V. D. Werth, R. M. Lieder, H. Jäger, H. Kämmerling, D. Kutchin, K. H. Maier, M. Berst, D. Gutknecht, and R. Henck, Prog. Part. Nucl. Phys. **28**, 495 (1992).
[8] T. Kuroyanagi, S. Mitarai, S. Suematsu, B. J. Min, H. Tomura, J. Mukai, T. Maeda, R. Nakatani, G. Sletten, J. Nyberg, and D. Jerrestam, Nucl. Instrum. Methods Phys. Res. A **316**, 289 (1992).
[9] J. J. Kolata, J. W. Olness, and E. K. Warburton, Phys. Rev. C **10**, 1663 (1974).
[10] J. Britz, A. Chevallier, J. Chevallier, and B. Haas, Nucl. Phys. **A262**, 189 (1976).
[11] C. A. Ur, Ph.D. thesis, University of Bucharest, 1998.
[12] C. D. O'Leary, M. A. Bentley, D. E. Appelbe, R. A. Bark, D. M. Cullen, S. Ertürk, A. Maj, J. A. Sheikh, and D. D. Warner, Phys. Lett. B **459**, 73 (1999).
[13] W. Kutschera, B. A. Brown, and K. Ogawa, Riv. Nuovo Cimento **1**, 1 (1978).
[14] W. A. Richter, M. G. van der Merwe, R. E. Julies, and B. A. Brown, Nucl. Phys. **A523**, 325 (1991).
[15] S. T. Hsieh, X. Ji, R. Mooy, and B. H. Wildenthal, in *Nuclear Structure at High Spin, Excitation and Momentum Transfer*, edited by H. Nann, AIP Conf. Proc. No. 142 (AIP, New York, 1986), p. 357.
[16] M. Sakakura, A. Arima, and T. Sebe, Phys. Lett. **61B**, 335 (1976).
[17] Th. Andersson, D. Rudolph, C. Baktash, J. Eberth, C. Fahlander, D. Haslip, D. R. LaFosse, S. D. Paul, D. G. Sarantites, C. E. Svensson, H. G. Thomas, J. C. Waddington, W. Weintraub, J. N. Wilson, and B. A. Brown, Eur. Phys. J. A **6**, 5 (1999).
[18] M. M. Hindi, J. H. Thomas, D. C. Radford, and P. D. Parker, Phys. Rev. C **27**, 2902 (1983).
[19] D. C. Zheng, L. Zamick, and D. Berdichevsky, Phys. Rev. C **42**, 1004 (1990).